Soft Matter

Accepted Manuscript

This article can be cited before page numbers have been issued, to do this please use: R. Paul, T. Ghosh, T. Tang and A. Kumar, *Soft Matter*, 2019, DOI: 10.1039/C9SM00794F.

ROYAL SOCIETY OF CHEMISTRY

rsc.li/soft-matter-journal

View Article Online
DOI: 10.1039/C9SM00794F

Rivalry in *Bacillus subtilis* Colonies: Enemy or Family?

Rajorshi Paul[1], Tanushree Ghosh[1], Tian Tang[1], Aloke Kumar[2*]

[1]Department of Mechanical Engineering, University of Alberta, Edmonton, Canada.

[2]Department of Mechanical Engineering, Indian Institute of Science, Bangalore, India.

***Corresponding author email:** alokekumar@iisc.ac.in

Abstract. Two colonies of *Bacillus subtilis* of identical strains growing adjacent to each other on an agar plate exhibit two distinct types of interactions: they either merge as they grow or demarcation occurs leading to formation of a line of demarcation at the colony fronts. The nature of this interaction depends on the agar concentration in the growth medium and the initial separation between the colonies. When the agar concentration was 0.67% or lower, the two sibling colonies were found to always merge. At 1% or higher concentrations, the colonies formed a demarcation line only when their initial separation was 20 mm or higher. Interactions of a colony with solid structures and liquid drops have indicated that biochemical factors rather than presence of physical obstacles are responsible for the demarcation line formation. A reaction diffusion model has been formulated to predict if two sibling colonies will form a demarcation line under given agar concentration and initial separation. The model prediction agrees well with experimental findings and generates a dimensionless phase diagram containing merging and demarcation regimes. The phase diagram is in terms of a dimensionless initial separation, $\bar{d}$, and a dimensionless diffusion coefficient, $\bar{D}$, of the colonies. Demarcation of the two interaction regimes can be described by a power law relation between $\bar{d}$ and $\bar{D}$.

View Article Online
DOI: 10.1039/C9SM00794F

1 Introduction

Bacterial colonies are excellent examples of active soft matter, where individual cells interact with each other as well as the external environment through physical and biochemical stimuli [1-4]. Inside these bacterial colonies bacterial cells can interact with each other using mechanisms that operate over several different length and time scales [5], by means of intercellular signaling [6-11], such as quorum sensing [12-14] as well as by production of biofilms and other extracellular materials [15-17]. Intercellular coordination in a colony allows bacteria to swarm on agar plates to derive nutrition from growth medium [18-22], produce fruiting bodies and sporulation [23, 24], and ensure their survival against external threats and adverse environmental conditions [25-27]. Bacterial colonies are equipped with a myriad of intricate defense strategies to protect themselves from predators, compete for limited resources as well as adapt and respond to outside stimuli [25, 28]. Interestingly, cues from the external environment can bring about measurable changes in the growth of bacterial colonies; changes in bacterial colonies due to such factors comprise an important domain of biophysical research [5].

When multiple bacterial colonies grow in close proximity, they interact with each other to compete for limited resources present in the growth medium. By means of biochemical sensing, bacteria can identify the neighbor colonies as enemy or family [1, 29-31], and this identification can affect their biophysical responses such as growth pattern, growth rates and the way they interact with the neighbor. Three distinct types of inter-colony interactions have been studied: between (a) different species of bacteria, (b) different strains of the same species, and (c) identical strains. Patra et al. and Chakraborty et al. studied the first case, i.e., the interaction between colonies of two different species of bacteria. They reported the formation of a demarcation line (DL) between two competing colonies [32, 33]. The interaction between colonies of two different strains

View Article Online
DOI: 10.1039/C9SM00794F

of the same species has been studied for *Proteus mirabilis* [34]. Two neighboring colonies of distinct strains of *P. mirabilis* have been reported to form a DL based on distinction between self and non-self [29, 34-38]. Interestingly, when identical strains of *P. mirabilis* are grown in proximity, the colonies merge and do not form a DL [29]. In point of fact, when colonies of same species (i.e. sibling colonies) interact, one may observe either a complete merging of the colonies (as in *P. mirabilis*), or formation of a DL, or in some cases, both. Sibling colonies of certain strains of *Paenibacillus dendritiformis* have been found to form DL [4]. Sibling *Bacillus subtilis* colonies exhibit both interaction behaviors under different nutrient conditions: DL form on nutrient deficient agar plates [39], while merging occurs in nutrient rich environments [40]. In a similar study, by varying the concentrations of agar and nutrients in the growth medium, Sekowska et al. observed both interactions in sibling colonies of *B. subtilis*, *Pseudoalteromonas haloplanktis*, *Salmonella typhimurium*, and *Escherichia coli* [41]. The interaction between sibling colonies is biologically distinct from the preceding cases, but has not been examined in detail. The fact that sibling colonies exhibit two marked behaviors makes the phenomenon a very interesting one, and is the subject of investigation in this work.

The nature of interaction between two sibling colonies may be governed by a number of biochemical and physical factors. Biochemical factors include the substrate which acts the nutrient source, the species of bacteria taking part and the mutation in these species. These factors influence the growth of bacterial colonies and are, thereby, expected to affect their interactions. On the other hand, spreading of bacterial colonies has been found to be dictated by physical factors such as osmotic pressure [42-44], surface tension [17, 45-48], permeability and viscous drag of the growth medium [49]; these may be influenced by the concentration of agar and nutrients, and the bacterial strain used. To understand the dynamics of inter-colony interactions,

View Article Online
DOI: 10.1039/C9SM00794F

it is necessary to study the role of these physical and biochemical factors. To date, the mechanism governing the duality in the interactions between sibling colonies is not very well understood. Sekowska et al. [41] found that the interaction between sibling colonies may be driven solely by the distribution of nutrients in the growth medium and DL may be formed when regions between colonies are depleted of nutrients. Espeso et al., studying DL formation in sibling *Pseudomonas putida* colonies, identified the rheology of the growth medium, and not the concentration of nutrients, to be the limiting factor in DL formation [38]. According to their study, DL formation is brought about by mechanical stresses resulting from the medium being compressed by the expanding colonies. Studies on colony interactions by Be'er et al. [4, 28, 50, 51] found that certain biochemical inhibition factors produced by the interacting sibling colonies are responsible for cell death, leading to DL formation. Esposo et al. and Be'er et al. showed that the concentration of agar and initial separation between inoculated colonies influence the front propagation of the sibling colonies [4, 38], but their exact roles were not studied in detail. Investigating the roles of these physical parameters in the interaction of multiple sibling bacterial colonies can be expected to yield insights into the spreading dynamics of bacterial soft matter, and yet an exhaustive understanding remains largely unexplored.

To address these scientific questions, we study how agar concentration and initial separation between two sibling *B. subtilis* colonies influence the nature of interaction between them. Agar concentration controls the radial spreading of each colony whereas the initial separation between the colonies signifies their maturity when they start interacting. *B. subtilis* is known to possess swimming and swarming motility which enable the bacteria to move quickly through semi-solid agar media [52, 53]. Systematic experiments are performed by varying the agar concentration and initial colony separation to generate an experimental phase diagram which

View Article Online
DOI: 10.1039/C9SM00794F

examines the conditions in which each interaction pattern emerges. To complement the experimental study, a reaction-diffusion model is established to predict the interaction patterns: merging and demarcation. Good agreement between our model and experiments allows us to generate a phase diagram that quantitatively describes the merging and demarcation of the *B. subtilis* colony interactions.

2 Methods

2.1. Materials and Microorganism

Miller's Luria Broth (LB) base (Bector, Dickinson and Company, 241420, containing 10 g/L pancreatic digest of casein, 5 g/L yeast extract and 0.5 g/L sodium chloride) was purchased from Fisher Scientific, Canada. Bacteriological agar was purchased from Sigma-Aldrich (A5306-250G, Canada). Bacterial strains *Bacillus subtilis* (ATCC© 6633) and *Escherichia coli* (ATCC© 25922) were purchased from American Type Culture Collection (ATCC©), Manassas, USA. Another bacterial species *Pseudomonas fluorescens* (CHA0) was generously given by Dr. Howard Ceri, Biofilm Research Group, Department of Biological Sciences, University of Calgary.

Polydimethylsiloxane (PDMS, Sylgard 184, Dow Corning, NY, USA) and Polypropylene (PP, cut out from Thermo Fisher Scientific Centrifuge Tubes) were used to fabricate cuboid and circular discs as substitutes for one of the colonies. The dimensions of the PDMS cuboid structures were 24 mm x 6 mm x 3 mm, and for PP, they were 30 mm x 5 mm x 1 mm. The diameter of the PDMS discs was 10 mm and height was 3 mm. For the PP discs, the diameter and height were 10 mm and 5 mm respectively. Commercial castor oil was used as a liquid substitute for a bacterial colony. Castor oil is highly viscous and has a molecular weight of 927

View Article Online
DOI: 10.1039/C9SM00794F

g/mol. Therefore, there is negligible diffusion of a sessile castor oil droplet on agar medium and they were used to simulate a static fluidic impediment for the growing bacterial colony. 1 μL of castor oil droplets were drop casted on the surface of agar on petri-dishes.

2.2. Preparation of growth medium

Miller's Luria Broth (LB) base was mixed with bacteriological agar to prepare a soft, nutrient rich medium for B. subtilis colony growth. Throughout the study, the concentration of LB in the growth medium was held constant (1.5%) while the concentration of agar was varied from 0.5% to 5% (w/v). The LB-agar solution was then autoclaved to prepare a sterile homogenous growth medium. The mixture was then poured to petri-dish (diameter 90 mm) and cooled down to room temperature before bacterial inoculation.

2.3. Bacterial culture preparation

For each experiment, a fresh pre-culture of the *B. subtilis* was prepared in 1.5% LB broth and incubated for 16 hours. The incubation temperature was maintained at 37°C for *B. subtilis* and *E. coli* cultures, while 30°C for *P. fluorescens*. Each bacterial colony was then prepared on an LB-agar plate by drop casting of 1μL of bacterial culture, and incubated at corresponding incubation temperatures. To maintain the bacterial cell density, the inoculum size was controlled by cell count. For *B. subtilis*, every 16-hour pre-culture contains 1.4×10^6 viable cells/ml with an optical density (at 600 nm) of 0.6 ± 0.02. The experimental deviation on cell count is calculated to be 0.4×10^6 in 1 ml which represents ~28% of the uncertainty in the repeatability of *B. subtilis* cell count. It can be assumed that the experimental inoculum (1μL) contained around 1×10^3 viable cells.

View Article Online
DOI: 10.1039/C9SM00794F

2.4. Experimental Design

Three different sets of experiments were performed to study radial growth pattern with *B. subtilis* during - i) two sibling colony interaction; ii) no interaction (single colony radial growth pattern) and iii) interaction with a physical object such as PDMS and castor oil. The first involved inoculating two sibling *B. subtilis* colonies on an agar plate. The concentration of agar in the growth medium was varied from 0.5% to 5% (w/v). During inoculation of the colonies by drop casting, we varied the distance between the centers of the drops in steps of 10 mm from 10 mm to 30 mm. This initial separation between the colonies and the concentration of agar in the growth medium were chosen as two parameters for our experiments. In the second set of experiments, a single colony was used to study the radial growth rate of *B. subtilis* colonies as a way to determine the diffusion coefficient of *B. subtilis* on agar when physical and biological interaction is absent. The concentration of agar was also varied between 0.5 and 5% (w/v). To collect data at equal intervals of time, two parallel sets of experiments were conducted, which were inoculated 12 hours apart. The third set of experiments was performed to study the interaction of *B. subtilis* colonies with physical objects. A sessile castor oil droplet as a liquid substitute, and PDMS and PP walls and discs as solid substitutes were used for replacing one of the sibling colonies. A *B. subtilis* colony was inoculated at a distance of 10 mm from the nearest edge of the sessile oil drop or PDMS/PP wall or disc. In these experiments, agar concentration was fixed at 1.5% (w/v). In all three sets of experiments, the nutrient concentration in the growth media was held constant at 1.5% (w/v) (or 15 g/L). Experimental observations were found to be sensitive to the changes in experimental conditions but under identical protocols they were

View Article Online
DOI: 10.1039/C9SM00794F

reasonably repeatable. Comments on experimental repeatability can be found in section I of the Supplementary Information.

2.5 Data collection and analysis

The growing bacterial colonies were recorded using a Nikon D3400 digital single-lens reflex (DSLR) camera with an 18-55 mm lens mounted on a tripod stand. The background illumination was provided using intensity adjustable 4" x 4" white LED backlight (Edmund Optics, Stock# 88-504). The petri-dishes were monitored at regular intervals of time to generate a uniform set of data. Microscopic images of the growing colonies were taken using a Nikon Eclipse Ti inverted microscope. The images were processed in MATLAB® (MathWorks®), using the inbuilt image processing toolbox, to obtain the size of the colonies.

The diffusion coefficient of the nutrient, a parameter required in the theoretical model, was estimated using Coomassie blue dye which has a molecular weight of 826 g/mol. 1 μL of the dye was allowed to spread on the surface of the growth medium on a petri-dish. Since the thickness of the agar in the petri-dish is insignificant compared to the diameter of the petri-dish (~4%), the dye diffusion is assumed to occur only on the agar surface. The intensity of color of the spreading dye was used as the indicator of dye concentration in the image processing. For estimating the growth parameters of *B. subtilis*, Origin® (OriginLab®) was used to fit the experimental growth curve with the theoretical model.

3 Results

3.1 Two Interaction Patterns

Figure 1 shows examples of two distinct interaction patterns observed under different conditions. When the concentration of agar was increased from 0.5% to 5% while keeping the separation

View Article Online
DOI: 10.1039/C9SM00794F

between two sibling colonies, *d*, at 20 mm, the sibling colonies change from merging into a single colony (Figures 1a), to forming a DL between the advancing colony fronts (Figure 1b). At sufficiently low agar concentrations ($\leq 0.67\%$), merging was observed in all cases when *d* was increased from 10 mm to 30 mm (Figure 1a; also see Supplementary Video 1 and 2). At higher agar concentrations ($\geq 1\%$), both merging and DL formation were observed by varying *d*, with the former occurring at small *d* (Figure 1c) and the latter at large *d* (Figure 1b; also see Supplementary Video 3). Section VIII of the Supplementary Information shows images of colonies interacting with each other at different combinations of *d* and the agar concentration.

As the interaction patterns in sibling *B. subtilis* colonies are affected by agar concentration and initial separation between the colonies, it is reasonable to propose that the underlying mechanism leading to DL formation is also influenced by these parameters. In fact, the agar concentration can impact the radial growth of the colonies, as demonstrated by our single colony experiments shown in Figure 2. Figure 2a shows the effective diameters of single *B. subtilis* colonies vs. the reciprocal of agar concentration, compared among several time points post inoculation. Figure 2b plots the effective colony diameters against time for three different agar concentrations. The mathematical model indicated in Figure 2b will be explained in the subsequent section. The effective colony diameter d_{eff} is defined as the diameter of the circle which covers the same area as the colony, $d_{eff} = \sqrt{\frac{4A}{\pi}}$, where A is the area covered by the colony. At 6 hours post inoculation, all colonies have similar diameters. But over time, the colony growing on 0.5% agar spreads at much faster rate, and the slowest growth is recorded on 2% agar. The influence of agar concentration on the rate of radial spreading of the colonies implies that it affects the biochemical sensing between the colonies, which occurs by exchange

View Article Online
DOI: 10.1039/C9SM00794F

and detection of specific molecules. Therefore, the onset of inter-colony repulsion that results in DL formation are influenced by the agar concentration. By affecting the colony spreading, agar also implicitly controls the state of maturity of the bacterial colonies at the time of interaction [42], which may contribute to the nature of interaction. Supplementary video 4 shows a magnified view of the spreading of colonies on 0.5% and 2% agar and how colonies mature over time.

Inoculated colonies start out as an aggregation of swimming bacteria present in the culture medium. Over time, an extracellular polymeric matrix is produced which facilitate motility, exchange of nutrients, water and other molecules from the growth medium [54]. The colonies mature by initially swelling and spreading outwards. The characteristics of colonies during different stages of the maturation process vary [5]. Therefore, the parameter d controls the stage of maturation the colonies are in when they start interacting with each other. Smaller separations mean that colonies start interacting very early into their maturation states. When d = 10 mm, colonies start merging at 14 hours post inoculation or earlier. For larger d, colony interaction starts after around 24 hours when agar concentration is high ($\geq 1\%$). Hence, the parameter d contributes to the how colonies interact with each other. A parametric investigation of the formation of DL (or its lack of) was performed experimentally and comparison made to a mathematical model that quantitatively describes the effects of agar and initial separation. The model will be discussed first followed by the comparison of a colony interaction phase diagram from both experiments and the model.

3.2 Mathematical Model

The complex living nature of the colonies makes it difficult to formulate a comprehensive mathematical model to govern the growth and dispersion of the micro-organisms in a colony.

View Article Online
DOI: 10.1039/C9SM00794F

Reaction-diffusion (RD) models have been a popular choice for modelling growing colonies because of their simplicity in describing a complex problem [32, 33, 55]. RD models typically assume that the colony consists of a network of cells which are continuously proliferating and spreading along the solid substrate (agar-based growth medium) driven by the necessity for nourishment. Bacterial population growth constitutes the reaction term. Bacterial spreading occurs by biased random walk of the cells [21] in response to an external impulse (chemicals [56], temperature [57], light [58], gravity [59]). This kind of movement can be captured by a diffusion term with a diffusion coefficient that depends on a wide range of factors such as bacterial density, propagation speed, chemical gradients and other growth conditions [55]. As the bacteria spread out radially on the agar surface, they metabolize the nutrients in the growth medium, creating a nutrient gradient. This results in simultaneous consumption and transport of the nutrients. To date, most of the RD models have, with reasonable success, been able to reproduce complicated morphologies exhibited by a single colony growing on a solid agar surface [55, 60-63]. Despite the substantial literature on modelling single bacterial colonies, very few models have attempted to investigate the interaction between multiple colonies. In addition, the existing models only explored a particular type of interaction, i.e. either DL formation [32, 33, 50] or merging [40]. In the present study two sibling colonies exhibit both interactions, therefore we would need a unified mathematical model capable of reproducing both patterns. Such a model needs to properly capture the growth of individual colonies as well as the interaction between two colonies, which will be discussed below.

First, we establish the nutrient dependent reaction diffusion equations for a single bacterial colony. The starting point is the classical Monod's nutrient depletion model [64] which describes the bacterial population demographics in a homogenous culture solution:

View Article Online
DOI: 10.1039/C9SM00794F

$$\frac{dX}{dt} = g(c)X \tag{1}$$

$$\frac{dc}{dt} = -\gamma g(c)X \tag{2}$$

Here, $X(t)$ and $c(t)$ are respectively the population density and the nutrient concentration in the solution. The constant γ is the yield which depicts the quantity of nutrient consumed for unit biomass generation. The specific growth rate $g(c)$ is dependent on the nutrient concentration by $g(c) = g_0 \frac{c}{k+c}$, where g_0 is the maximum specific growth rate which signifies the specific growth rate in a nutrient rich environment $(c \to \infty)$, and k is the half-saturation constant. Equation (1) accounts for growth of bacterial population by metabolizing nutrients. This equation is coupled with the nutrient consumption equation (equation (2)). In the Monod's model, the rate of nutrient consumption is assumed to be proportional to the rate at which population increases, with the constant of proportionality being the yield γ. The growth parameters γ, g_0 and k depend on the initial concentration of bacteria in solution, concentration and type of nutrients, conditions of growth including temperature, pH, as well as the species of bacteria in the solution. For modelling colony growth on agar surfaces, equations (1) and (2) are modified to take into account the spreading of bacteria on agar based semi-solid growth media. The radial spreading can be accurately modelled as a diffusion process driven by chemotaxis [55]. The concentration of agar in the growth medium is high enough that the bacteria spread only along the surface by swarming and do not penetrate the growth medium [19]. Therefore, the dispersion of the bacteria is two-dimensional. As discussed before, the diffusion coefficient which describes bacterial motility generally depends on a wide range of parameters, out of which, the concentrations of agar and nutrient are relevant to the present study. The influence of

View Article Online
DOI: 10.1039/C9SM00794F

nutrient concentration on the diffusion coefficient is first examined. Bacterial cells propagate by expending energy derived from nutrient metabolism. In nutrient deficient environments, the motility of cells will, therefore, be impaired [41, 65]. To account for the nutrient dependence of bacterial motility, Patra et al. proposed the use of Heaviside step function to define a threshold nutrient concentration [33] c^*. Thus, for a single bacterial colony, the nutrient dependent reaction-diffusion can be represented as follows:

$$\frac{\partial X}{\partial t} = g(c)X + \nabla \cdot \left(D_b \mathcal{H}\left[c - c^* \right] \nabla X \right) \tag{3}$$

$$\frac{\partial c}{\partial t} = -\gamma g(c)X + \nabla \cdot \left(D_c \nabla c \right) \tag{4}$$

Here, D_b and D_c are the diffusion coefficients of the colony and the nutrient respectively. c^* is the threshold nutrient concentration below which bacterial motility is assumed to be absent, and $\mathcal{H}\left[x\right]$ is the Heaviside step function. The colony growth and spreading are governed by equation (3), whereas equation (4) accounts for nutrient consumption and transport. As discussed previously, the reaction terms in equations (3) and (4) describe the bacterial proliferation and nutrient consumption respectively. The diffusion terms, on the other hand, account for bacterial dispersion and diffusion of nutrients on the surface of agar. For the single colony model, it is assumed that the Monod growth parameters for the bacteria in the agar medium will be identical to those growing in liquid culture media. Therefore, these parameters are estimated from *B. subtilis* growth curves generated in LB liquid culture as indicated in Figure S1 (see Supplementary Information section I). The single colony model is necessary to estimate the diffusion coefficient of the colony, D_b. As the rate of radial spreading of the colonies depend on the concentration of agar in the growth medium, equation (3) allows us to determine D_b as a

View Article Online
DOI: 10.1039/C9SM00794F

function of the agar concentration, so as to incorporate the influence of agar into our mathematical model in terms of D_b.

To study the dynamics of two sibling colonies, one can append the single colony model by incorporating a term which captures the inter-colony interactions into the model. Such interaction is manifested in terms of cell death at the advancing colony fronts [4, 50, 66], as given by equations (5) - (7):

$$\frac{\partial X_1}{\partial t} = g(c)X_1 + \nabla\cdot\left(D_b\mathcal{H}\left[c-c^*\right]\nabla X_1\right) - m(t) \tag{5}$$

$$\frac{\partial X_2}{\partial t} = g(c)X_2 + \nabla\cdot\left(D_b\mathcal{H}\left[c-c^*\right]\nabla X_2\right) - m(t) \tag{6}$$

$$\frac{\partial c}{\partial t} = -\gamma g(c)X + \nabla\cdot\left(D_c\nabla c\right) \tag{7}$$

Here, X_1, X_2 are the population densities of the individual colonies, and $X = X_1 + X_2$ is the net population density. The mortality rate $m(t)$ captures the inter-colony interaction, and is dependent on the population of both sibling colonies. In this model, the two colonies are assumed to be identical to each other, and hence the same model parameters, including Monod's growth parameters and diffusion coefficients will be used for both colonies. Furthermore, it is also assumed that these parameters will be the same as those for a single colony, i.e., growth characteristics are unaffected because of inter-colony interactions. In the proposed model, it is assumed that the interaction between the sibling colonies is antagonistic in nature, where each sibling colony brings about death of cells of the rival colony at the approaching colony fronts. This is motivated by the experimental observation of Be'er et al. [4, 28, 50]. We assume that mortality occurs only in presence of an invading colony. Single colonies growing independently do not experience cell mortality on their own. Therefore, the mortality term is absent in the single colony model. To model the interactions between two sibling colonies, we assume $m(t)$

View Article Online
DOI: 10.1039/C9SM00794F

to be proportional to the population of both colonies, i.e., $m(t) = \mu X_1 X_2$ where μ is the mortality coefficient [33] which is assumed to be a constant in the present study. The advantage of defining the mortality rate this way is that in the initial stages of growth, the sibling colonies grow independently and $m(t) = 0$. The mortality term is active only near the DL where the two colonies interact and is zero elsewhere. This definition of mortality, however, means that whenever the sibling colonies interact, the cell death at the colony fronts will produce a stable interface [33]. This is not consistent with our experimental findings. Our experiments show that in the cases with DL formation, lines started forming ~24 hours after incubation. However, the colonies which merged were found to start merging much earlier (at around 20 hours or earlier; see Supplementary Videos 1, 2 and 3). This temporal disparity can be explained in terms of the different rates of colony propagation on growth media with varied agar concentration (Figure 2). At higher concentrations of agar (>1.5%), colonies have been found to propagate at a slower pace. Consequently, in such conditions colonies start interacting with each other at a later time as compared to colonies which spread faster on media with lower agar concentration. According to the study by Be'er et al., biochemical inhibition occurs only when the concentration of the inhibition factors reaches a threshold concentration [4]. Therefore, in the event that the DL formation is brought about by biochemical inhibition, it is reasonable to assume that the diffusing biochemical factors reach the lethal concentration at a certain instant of time after which the interacting colonies start exhibiting cell mortality leading to DL formation. It is likely that the difference in time scales observed in the experiments is related to the time at which the inhibition factors reach lethal concentration. To account for this time delay in the onset of demarcation and merging, we introduce a reference time t^* before which cell death does not initiate. This can be achieved by using a time-dependent step function, $m(t) = \mu X_1 X_2 \mathcal{H}\left[t - t^*\right]$.

View Article Online
DOI: 10.1039/C9SM00794F

A detailed analysis of the physical significance of t^* is available in Section V of Supplementary Information. The mortality rate in this form can generate both merging and demarcation interactions. However, simulations show that when colonies which initially merge when $t < t^*$ eventually separate and start repelling each other when the mortality term is activated at $t > t^*$. This is not consistent with experiments which showed that after two colonies merged, they continued to grow as a single unit. In recognition of this observation, a second step function is introduced so that the final expression for the mortality rate is given by:

$$m(t) = \mu X_1 X_2 \mathcal{H}\left[t - t^*\right] \mathcal{H}\left[X_e - X\left(t, x = 0, y = 0\right)\right] \tag{8}$$

$X\left(t, x = 0, y = 0\right)$ is the net population density midway between the centers of two colonies located at the coordinates $x = 0, y = 0$ (see Figure 3). X_e is a cut-off population density which demarcates the edge of each colony. The second Heaviside function checks the population midway between the sibling colonies. If the population exceeds the cut-off population X_e at any time, colonies have merged, and the step function suppresses the mortality term so that colonies continue to grow as a single unit. Otherwise, the mortality term is activated, and a stable DL is generated numerically. It is to be noted that the mortality rate is a function of both time and space coordinates. Its effect is felt only at the midway between the two colonies where the DL forms, while the temporal dependence of the function is of key importance. Hence, for the sake of simpler notation, we have omitted the notation for space dependence and denote the mortality rate by $m(t)$.

The established RD equations, equations (5) - (7) along with (8), are solved with appropriate initial and boundary conditions. Figure 3 shows the simulation domain at $t = 0$, when the nutrient

View Article Online
DOI: 10.1039/C9SM00794F

concentration in the medium is homogenous and the colonies are inoculated as sessile droplets of radius ρ with a separation of d, i.e.,

$$X_1\left(t=0,\left(x-\frac{d}{2}\right)^2+y^2\le\rho^2\right)=X_2\left(t=0,\left(x+\frac{d}{2}\right)^2+y^2\le\rho^2\right)=X_0$$
$$c\left(t=0,x,y\right)=c_0. \tag{9}$$

At the boundary of the rectangular domain (Γ), no flux boundary condition is enforced for the population densities and a constant nutrient concentration c_0 is assumed:

$$\nabla X_1\cdot\hat{\mathbf{n}}\big|_\Gamma=\nabla X_2\cdot\hat{\mathbf{n}}\big|_\Gamma=0$$
$$c\big|_\Gamma=c_0 \tag{10}$$

3.3 Numerical Results and Comparison to Experiments

Several parameters are required in solving the initial-boundary value problem proposed in section 3.2. The growth parameters, the diffusion coefficients and the reference time t^* depend on the bacterial species, composition of the nutrient and the experimental conditions which include the agar concentration and the bacterial biomass in the inoculum. As a result, these parameters are to be determined experimentally to be used in the mathematical model. The other model parameters are chosen based on experimental design and numerical stability within bounds of tenable physical significance.

The growth parameters in the Monod's model, namely g_0, k and γ, are estimated by comparing the model prediction of single colony growth in homogenous solution with the experimental growth curve (see Supplementary Information section II). By measuring the diffusion of Coomassie blue dye on the surface of agar plates, the diffusion coefficient of the nutrient, D_c, was estimated to be on the order of 10^{-3} mm^2/h (see Supplementary Information section III). The diffusion coefficient of colony on agar, D_b, was then calculated by comparing

View Article Online
DOI: 10.1039/C9SM00794F

the radial growth of the colony observed experimentally to the numerical result obtained by solving equations (3) and (4). Figure 2b shows a good match between the experiment and theory. In accordance with previous discussion, we have obtained very large D_b at 0.5% agar, nearly one order of magnitude higher than those estimated for the other agar concentrations (see Supplementary Information section IV). The estimates of the model parameters are summarized in Table 1.

Table 1. Estimates of Model Parameters

Parameters		**Estimate**
Bacterial Growth	g_0	4 h^{-1}
	γ	16 g/L
	k	42.5 g/L
Nutrient Diffusion	D_c	10^{-3} mm^2/h
Colony Dispersion	D_b	0.04 – 0.21 mm^2/h

Based on our experimental observations on the onset time of merging and DL formation, the reference time t^* is chosen as 20 h. The cut-off population density X_e chosen as $X_e = 0.3$. X_e depends on the initial condition X_0, and would be change if a different initial condition is used. Values of other parameters used in the simulations are: $\mu = 40\ h^{-1}$, $c^* = 1.5$ g/L. The value of μ is chosen to numerically generate a stable interfaced as $\mu = 40\ h^{-1}$. The value of the threshold nutrient concentration c^* does not have any notable influence on the numerical results and is arbitrarily chosen. The initial conditions are set to be $c_0 = 15$ g/L, and $X_0 = 10^{-3}$. The details on the methodology of choosing the values of the model parameters are provided in section V of Supplementary Information. The simulation domain is a 92 mm X 92 mm square with its center at the origin of the coordinate system. The colonies are inoculated at y = 0

View Article Online
DOI: 10.1039/C9SM00794F

symmetrically about the origin with a center-to-center separation of *d*. The radius of the inoculation droplet is taken as $\rho = 2.5$ mm. The coupled equations are solved using the second order Forward-Time Central-Space (FTCS) scheme. The rectangular simulation domain is decomposed into 369 x 369 grid points, with a grid resolution of 0.25 mm. Numerical solution is obtained between t = 0 and t = 48 hours, in steps of 34 sec (i.e., 5001 time steps).

The numerically simulated colony interactions are shown in Figure 4 for different values of the diffusion coefficient D_b and the initial separation d. To define the boundary of the colony from the continuous solution of the RD equations, reference population X_e is predefined. The value of X_e is chosen as $X_e = 0.3$. In Figure 4a, we see that colonies merge when the diffusion coefficient is 0.21 mm^2/h and d = 20 mm. The diffusion coefficient, in this case, is large and corresponds to very low agar concentrations (~0.5%) when bacteria are highly motile and the colonies spread rapidly. Experimentally, the conditions represent those in Figure 1a. When the diffusion coefficient is reduced by almost one order of magnitude to 0.04 mm^2/h without changing *d* (Figure 4b), we observe that a DL forms. This case depicts Figure 1b at 48 h. Finally, in Figure 4c, *d* is reduced to 10 mm while keeping the diffusion coefficient constant. Here, the colonies merge completely without any DL formation, as seen in Figure 1c. Therefore, we find a good qualitative agreement between the experiments and the proposed mathematical model.

The initial-boundary value problem in section 3.2 can also be non-dimensionalized (see details in Supplementary Information section VI), which allows us to identify two governing dimensionless parameters: a normalized separation $\bar{d} = d\sqrt{r_0 / D_c}$, and a normalized diffusion coefficient $\bar{D} = D_b / D_c$. Figure 5a shows a dimensionless phase diagram in the $\bar{d} - \bar{D}$ space where two distinct regimes underline the generalized conditions for whether two colonies would

View Article Online
DOI: 10.1039/C9SM00794F

form a DL or merge. To determine whether the colonies merge or form a DL numerically, we check the total population density midway between the centers of two colonies at an instant $t > t^*$. If $X\left(t > t^*, x = 0, y = 0\right) \geq X_e$, colonies merge, else a DL forms. For each value of $\bar{D}$, there exists a critical separation $\bar{d}^*$, where the nature of interaction changes from merging to DL. The relation $\bar{d}^* = f\left(\bar{D}\right)$ determines the boundary between the merging and DL regimes in the phase diagram. The function f can be well approximated as a power law relation where $\bar{d}^* = \alpha \bar{D}^n$, and α and n are numerical constants. α and n has been found numerically as: $\alpha = 276.6, n = 0.377$. From this simple empirical expression, we can now predict, with an acceptable degree of accuracy, the outcome of interaction between two sibling colonies given the initial separation and the diffusion coefficient (in extension, the agar concentration). A dimensional phase diagram is plotted in Figure 5b using a quadratic correlation between D_b and the inverse agar concentration (see Supplementary Information section IV). Figure 5b shows that when the separation is sufficiently small e.g., $d \leq 10$ mm, the sibling colonies would merge irrespective of the value of the agar concentration within the chosen range. The model also predicts that when the diffusion coefficient is sufficiently large, i.e., for very low agar concentrations, the colonies merge even when d is as high as 30 mm. The experimental phase diagram generated from two-colony experiments is superposed on the numerical phase diagram to compare the experimental and numerical results which shows a good agreement. In the phase diagrams shown in Figure 5, the phase boundary separates the regions where the behavior of colonies changes from being "family" (in red) to "enemy" (in blue). Therefore, we will refer to the phase boundary denoted by the power law relation as the "*Laxman Line*" (based on the Laxman Rekha described in the Indian epic, the Ramayana).

View Article Online
DOI: 10.1039/C9SM00794F

The exponent n in the empirical relation $\bar{d}^* = \alpha \bar{D}^n$ has some interesting implications. Figure 5c plots $\bar{d}^*$ against $\bar{D}$ for different values of the exponent, while keeping the coefficient $\alpha = 276.6$ as constant. On increasing the value of n from 0.377 to 0.5, the boundary line separating the two phases becomes steeper and $\bar{d}^*$ increases for the same $\bar{D}$. This means that the sibling colonies would be more susceptible to merging. On the other hand, on decreasing n from 0.377 to 0.2, the boundary line becomes flatter and shifts downwards, which signifies that the colonies would tend to form DL. Physically, one can expect n to be large in bacterial species which are known to merge such as identical strains of *P. mirabilis*. Bacterial species such as *E.coli* (Figures 6a and 6b) tend to form a DL between sibling colonies when they interact. For such species, we would expect the exponent n to be small.

The exponent n is found to be dependent on the model parameter t^*, as shown in Figure 5d. On increasing the value of t^*, the estimated value of n is found to increase, when all other model parameters are maintained constant. Physically, increasing t^* delays the onset of demarcation which means that colonies are more susceptible to merging than demarcation. Based on previous discussion, this indicates that the exponent n will also increase. The numerical data in Figure 5d is fitted with an exponential function $n = 0.41\left(1 - 1.53e^{-0.15t^*}\right)$. The quality of fit measured in terms of the coefficient of determination is $R^2 = 99.8\%$.

4 Discussions

Our experiments have shown that the concentration of agar influences the rate of spreading of *B. subtilis* colonies. Agar-based growth media that are generally used for micro-biological studies are essentially hydrogels. They are porous, and the size of the pores depends on the

View Article Online
DOI: 10.1039/C9SM00794F

concentration of agar [67]. At very low concentrations ($\leq 0.67\%$), the agar medium is soft and holds a large proportion of water. In such conditions, the bacteria can swarm rapidly on the surface and derive nutrition from the growth medium. As the concentration of agar is increased from 0.5%, the proportion of water in the medium commensurately decreases and the hydrogel becomes harder. Hard and dry agar surface is unfavourable towards bacterial motility and the colonies spread slowly. On 0.5% agar, due to rapid swarming, the colonies experience less competition in procuring nutrient and consequently are found to merge with sibling colonies even when d is as large as 30 mm [41]. This is, however, not true for higher agar concentrations. The unfavourable condition of the growth medium may trigger inter-colony repulsion as a defense mechanism and thereby lead to DL formation when d = 20 mm or higher.

The duality of DL and merging is not specific to *B. subtilis*. While *B. subtilis* is a Gram-positive bacterium, our experiments with Gram-negative *Pseudomonas fluorescens* showed that this phenomenon is a general one exhibited by multiple species of bacteria (see Figures 6a for examples).

The advancing fronts of sibling colonies are physical obstacles in the progression of the colonies. It is possible that the sibling colonies act as mutual physical deterrence and prevent merging in high agar concentrations and/or when the colonies are relatively far apart. To see if DL formation is induced by the presence of physical barriers, we simulated one of the colonies with a physical object (liquid: castor oil droplet or a solid structure: PDMS and PP walls and discs) and let a *B. subtilis* colony grow adjacent to the physical object. PDMS and PP are commonly used solid substrates in bacteriological studies and are known to be compatible with bacterial growth [53, 68-71]. The solid PDMS and PP structures were created in the form of a flat wall (to simulate a flat DL formed between sibling colonies as in Figure 1b) and a circular disc

View Article Online
DOI: 10.1039/C9SM00794F

(to represent a growing colony). Figure 7 shows how the *B. subtilis* colonies interact with these physical obstacles (see section VII of Supplementary Information for detailed results). In all four cases, we observe the colonies growing along the edge of the physical structures showing no signs of DL formation. The separations between the colonies and the physical barriers have been so chosen that at these separations, DL formation has been observed in two colony experiments but is absent here. The experiments clearly show that the presence of a physical deterrence may not, by itself, lead to a DL being formed. Only when a sibling colony is present in the vicinity does a DL form under the appropriate combination of agar concentration and separation. This suggests that DL formation is not primarily dictated by physical factors, but rather biochemical factors are involved which is due to the presence of a sibling colony.

Several comments are made regarding the underlying assumptions and the limitation of the proposed mathematical model. The proposed model tries to reconcile the experimental observations of Sekowska et al. [41] and Be'er et al. [4, 28, 50]. In accordance with the study by Sekowska and co-workers, the present model shows that nutrient depletion occurs at a faster rate in regions between the sibling colonies. On the other hand, the model also incorporates a mortality term to account for the inter-colony repulsion, which is based on the experimental observation of Be'er et al. In the present work we do not investigate the mechanism governing the inter-colony interactions. Instead, we have defined a reference time t^* in the model, which is based on experiments. Our experiments with physical barriers have indicated that the sibling colony interactions occur by exchange of biochemicals. Therefore, an alternate to the proposed model would involve explicitly solving the transport equation for associated biochemicals. We have tried to formulate a generalized mathematical model to describe the dual interaction patterns that may be applicable to multiple species of bacteria (e.g. *Pseudomonas fluorescens*).

View Article Online
DOI: 10.1039/C9SM00794F

For this reason, we intentionally refrained from commenting on the underlying biochemical processes that lead to DL formation specific to *B. subtilis* (e.g. sporulation). We have used an order of magnitude estimate of the nutrient diffusion coefficient and assumed it to be constant. In reality, however, the diffusion coefficient of the nutrient can be expected to vary with agar concentration.

5 Conclusions

In this work, we have investigated the influence of physical parameters in the inter-colony interactions in *B. subtilis*. To our knowledge, this is the first evidence of two sibling colonies forming two distinct interaction patterns: merging and DL formation, regulated by the agar concentration and the separation between colonies. From interactions in sibling *P. fluorescens* colonies, we have demonstrated that these dual interaction patterns constitute a general behavior in certain bacteria. We have found that a *B. subtilis* colony forms a DL only when an adjacent sibling colony is present, and not when a physical obstacle is present in the vicinity of the colony. This indicates that the DL formation is dictated by biochemical factors and is not influenced by presence of any physical deterrence. The phenomenon has been found to be governed by the agar concentration which affects the radial spreading of the colonies, and the separation between the colonies which indicates the maturity of the interacting colonies.

Based on the experimental observations, we have formulated a reaction-diffusion model to reproduce the interaction patterns in *B. subtilis*. A time dependent mortality rate has been defined to simulate both interactions: merging and DL formation using the same model, possibly the only existing mathematical model to do so. The effect of agar has been incorporated into the model in terms of the diffusion coefficient of the bacterial colony. A unique feature of our model

View Article Online
DOI: 10.1039/C9SM00794F

is that we have obtained non-dimensionless solution of the governing equations making our solution versatile and can be extended to other bacterial systems. The model generates a numerical phase diagram which separates the two interaction regimes in terms of the dimensionless separation $\bar{d}$ and the normalized diffusion coefficient $\bar{D}$. The numerical and experimental phase diagrams have been found to be in good agreement. The dimensionless critical separation $\bar{d}^*$ which demarcates the two regimes follows a simple power law relation, $\bar{d}^* = \alpha \bar{D}^n$. This allows us to predict the nature of interaction for a given combination of the parameters.

Acknowledgements

The authors are grateful to the Alberta Bio Future Research and Innovation Program, Alberta Innovates Bio Solutions, Government of Alberta, Canada for sponsoring the project. This research has been funded under the project title "Engineering lignin as a precursor for carbon fiber using novel biodegradation and purification techniques" (BFR032) headed by Dr. Tian Tang, Dr. Aloke Kumar and Dr. Cagri Ayranci (Mechanical Engineering, University of Alberta). We also thank Dr. Howard Ceri, University of Calgary for providing us *Pseudomonas fluorescens* strains for our experiments. Dr. Aloke Kumar also acknowledges partial support from DST-SERB grant no EMR/2017/003025.

View Article Online
DOI: 10.1039/C9SM00794F

References

1. J. A. Shapiro, *Sci Am*, 1988, **258**, 82-89.
2. E. Ben-Jacob, O. Schochet, A. Tenenbaum, I. Cohen, A. Czirok and T. Vicsek, *Nature*, 1994, **368**, 46-49.
3. E. Ben-Jacob, I. Cohen and D. L. Gutnick, *Annual Review of Microbiology*, 1998, **52**, 779-806.
4. A. Be'er, H. P. Zhang, E. L. Florin, S. M. Payne, E. Ben-Jacob and H. L. Swinney, *P Natl Acad Sci USA*, 2009, **106**, 428-433.
5. A. Karimi, D. Karig, A. Kumar and A. M. Ardekani, *Lab Chip*, 2015, **15**, 23-42.
6. D. Kaiser and R. Losick, *Cell*, 1993, **73**, 873-885.
7. D. Kaiser, *Science*, 1996, **272**, 1598-1599.
8. R. Wirth, A. Muscholl and G. Wanner, *Trends Microbiol*, 1996, **4**, 96-103.
9. E. Ben Jacob, I. Becker, Y. Shapira and H. Levine, *Trends Microbiol*, 2004, **12**, 366-372.
10. B. L. Bassler and R. Losick, *Cell*, 2006, **125**, 237-246.
11. S. B. von Bodman, J. M. Willey and S. P. Diggle, *J Bacteriol*, 2008, **190**, 4377.
12. M. B. Miller and B. L. Bassler, *Annual Review of Microbiology*, 2001, **55**, 165-199.
13. C. M. Waters and B. L. Bassler, *Annu Rev Cell Dev Bi*, 2005, **21**, 319-346.
14. K. Papenfort and B. L. Bassler, *Nat Rev Microbiol*, 2016, **14**, 576-588.
15. D. López and R. Kolter, *Fems Microbiol Rev*, 2010, **34**, 134-149.
16. E. Anne Shank and R. Kolter, *Curr Opin Microbiol*, 2011, **14**, 741-747.
17. R. De Dier, M. Fauvart, J. Michiels and J. Vermant, in *The Physical Basis of Bacterial Quorum Communication*, Springer, 2015, pp. 189-204.
18. R. F. Kinsinger, M. C. Shirk and R. Fall, *J Bacteriol*, 2003, **185**, 5627-5631.
19. D. B. Kearns and R. Losick, *Mol Microbiol*, 2003, **49**, 581-590.
20. A. Venieraki, P. C. Tsalgatidou, D. G. Georgakopoulos, M. Dimou and P. Katinakis, *Journal*, 2016, **9**, 16.
21. G. Ariel, A. Rabani, S. Benisty, J. D. Partridge, R. M. Harshey and A. Be'er, *Nat Commun*, 2015, **6**.
22. R. M. Harshey and J. D. Partridge, *J Mol Biol*, 2015, **427**, 3683-3694.
23. S. S. Branda, J. E. Gonzalez-Pastor, S. Ben-Yehuda, R. Losick and R. Kolter, *P Natl Acad Sci USA*, 2001, **98**, 11621-11626.
24. A. Driks, *Cell Mol Life Sci*, 2002, **59**, 389-391.
25. G. M. Dunny, T. J. Brickman and M. Dworkin, *Bioessays*, 2008, **30**, 296-298.
26. L. Chao and B. R. Levin, *P Natl Acad Sci-Biol*, 1981, **78**, 6324-6328.
27. V. C. Thomas and L. E. Hancock, *Int J Artif Organs*, 2009, **32**, 537-544.
28. A. Be'er, S. Benisty, G. Ariel and E. Ben-Jacob, in *The Physical Basis of Bacterial Quorum Communication*, ed. S. J. Hagen, Springer New York, New York, NY, 2015, DOI: 10.1007/978-1-4939-1402-9_8, pp. 145-162.
29. K. A. Gibbs, M. L. Urbanowski and E. P. Greenberg, *Science*, 2008, **321**, 256-259.
30. P. Stefanic, B. Kraigher, N. A. Lyons, R. Kolter and I. Mandic-Mulec, *P Natl Acad Sci USA*, 2015, **112**, 14042-14047.
31. N. A. Lyons, B. Kraigher, P. Stefanic, I. Mandic-Mulec and R. Kolter, *Curr Biol*, 2016, **26**, 733-742.
32. B. Chakraborty, A. Mallick, S. Annagiri, S. Sengupta and T. K. Sengupta, *R Soc Open Sci*, 2016, **3**, 160438.

View Article Online
DOI: 10.1039/C9SM00794F

33. P. Patra, C. N. Vassallo, D. Wall and O. A. Igoshin, *Biophys J*, 2017, **113**, 2477-2486.
34. A. E. Budding, C. J. Ingham, W. Bitter, C. M. Vandenbroucke-Grauls and P. M. Schneeberger, *J Bacteriol*, 2009, **191**, 3892-3900.
35. L. Dienes, *J Bacteriol*, 1946, **51**, 585.
36. L. Dienes, *Proceedings of the Society for Experimental Biology and Medicine*, 1947, **66**, 97-98.
37. B. W. Senior, *J Gen Microbiol*, 1977, **102**, 235-244.
38. D. R. Espeso, E. Martinez-Garcia, V. de Lorenzo and A. Goni-Moreno, *Front Microbiol*, 2016, **7**, 1437.
39. H. Fujikawa and M. Matsushita, *J Phys Soc Jpn*, 1991, **60**, 88-94.
40. J. Wakita, K. Komatsu, A. Nakahara, T. Matsuyama and M. Matsushita, *J Phys Soc Jpn*, 1994, **63**, 1205-1211.
41. A. Sekowska, J.-B. Masson, A. Celani, A. Danchin and M. Vergassola, *Biophys J*, 2009, **97**, 688-698.
42. A. Seminara, T. E. Angelini, J. N. Wilking, H. Vlamakis, S. Ebrahim, R. Kolter, D. A. Weitz and M. P. Brenner, *P Natl Acad Sci USA*, 2012, **109**, 1116-1121.
43. S. Trinschek, K. John and U. Thiele, *Aims Mater Sci*, 2016, **3**, 1138-1159.
44. J. Yan, C. D. Nadell, H. A. Stone, N. S. Wingreen and B. L. Bassler, *Nat Commun*, 2017, **8**, 327.
45. S. Trinschek, K. John, S. Lecuyer and U. Thiele, *Phys Rev Lett*, 2017, **119**.
46. W. J. Ke, Y. H. Hsueh, Y. C. Cheng, C. C. Wu and S. T. Liu, *Frontiers in Microbiology*, 2015, **6**.
47. A. Be'er, R. S. Smith, H. P. Zhang, E. L. Florin, S. M. Payne and H. L. Swinney, *J Bacteriol*, 2009, **191**, 5758-5764.
48. S. Trinschek, K. John and U. Thiele, *Soft Matter*, 2018, **14**, 4464-4476.
49. A. Yang, W. S. Tang, T. Y. Si and J. X. Tang, *Biophys J*, 2017, **112**, 1462-1471.
50. A. Be'er, G. Ariel, O. Kalisman, Y. Helman, A. Sirota-Madi, H. P. Zhang, E. L. Florin, S. M. Payne, E. Ben-Jacob and H. L. Swinney, *P Natl Acad Sci USA*, 2010, **107**, 6258-6263.
51. A. Be'er, E. L. Florin, C. R. Fisher, H. L. Swinney and S. M. Payne, *Mbio*, 2011, **2**.
52. A. Bridier, D. Le Coq, F. Dubois-Brissonnet, V. Thomas, S. Aymerich and R. Briandet, *Plos One*, 2011, **6**.
53. A. M. Kollaran, S. Joge, H. S. Kotian, D. Badal, D. Prakash, A. Mishra, M. Varma and V. Singh, *iScience*, 2019, **13**, 305-317.
54. M. G. Mazza, *J Phys D Appl Phys*, 2016, **49**.
55. I. Golding, Y. Kozlovsky, I. Cohen and E. Ben-Jacob, *Physica A*, 1998, **260**, 510-554.
56. R. M. Macnab and D. Koshland, *Proceedings of the National Academy of Sciences*, 1972, **69**, 2509-2512.
57. S. i. Nishiyama, T. Umemura, T. Nara, M. Homma and I. Kawagishi, *Mol Microbiol*, 1999, **32**, 357-365.
58. I. B. Zhulin, *Journal of molecular microbiology and biotechnology*, 2000, **2**, 491-494.
59. D.-P. Häder, in *Biophysics of Photoreceptors and Photomovements in Microorganisms*, Springer, 1991, pp. 203-221.
60. D. Schwarcz, H. Levine, E. Ben-Jacob and G. Ariel, *Physica D*, 2016, **318**, 91-99.
61. G. Book, C. Ingham and G. Ariel, *Plos One*, 2017, **12**.
62. H. Tronnolone, A. Tam, Z. Szenczi, J. E. F. Green, S. Balasuriya, E. L. Tek, J. M. Gardner, J. F. Sundstrom, V. Jiranek, S. G. Oliver and B. J. Binder, *Sci Rep-Uk*, 2018, **8**.

View Article Online
DOI: 10.1039/C9SM00794F

63. P. Patra, K. Kissoon, I. Cornejo, H. B. Kaplan and O. A. Igoshin, *Plos Comput Biol*, 2016, **12**.
64. J. Monod, *Annual Review of Microbiology*, 1949, **3**, 371-394.
65. M. P. Brenner, L. S. Levitov and E. O. Budrene, *Biophys J*, 1998, **74**, 1677-1693.
66. J. E. Gonzalez-Pastor, E. C. Hobbs and R. Losick, *Science*, 2003, **301**, 510-513.
67. J. Narayanan, J.-Y. Xiong and X.-Y. Liu, *Journal of Physics: Conference Series*, 2006, **28**, 83-86.
68. R. Iibuchi, Y. Hara-Kudo, A. Hasegawa and S. Kumagai, *J Food Protect*, 2010, **73**, 1506-1510.
69. N. Singh, V. Agrawal, S. C. Pemmaraju, R. Panwar and V. Pruthi, *Indian J Biotechnol*, 2011, **10**, 417-422.
70. A. Valiei, A. Kumar, P. P. Mukherjee, Y. Liu and T. Thundat, *Lab Chip*, 2012, **12**, 5133-5137.
71. A. Kumar, D. Karig, R. Acharya, S. Neethirajan, P. P. Mukherjee, S. Retterer and M. J. Doktycz, *Microfluid Nanofluid*, 2013, **14**, 895-902.

View Article Online
DOI: 10.1039/C9SM00794F

Figures

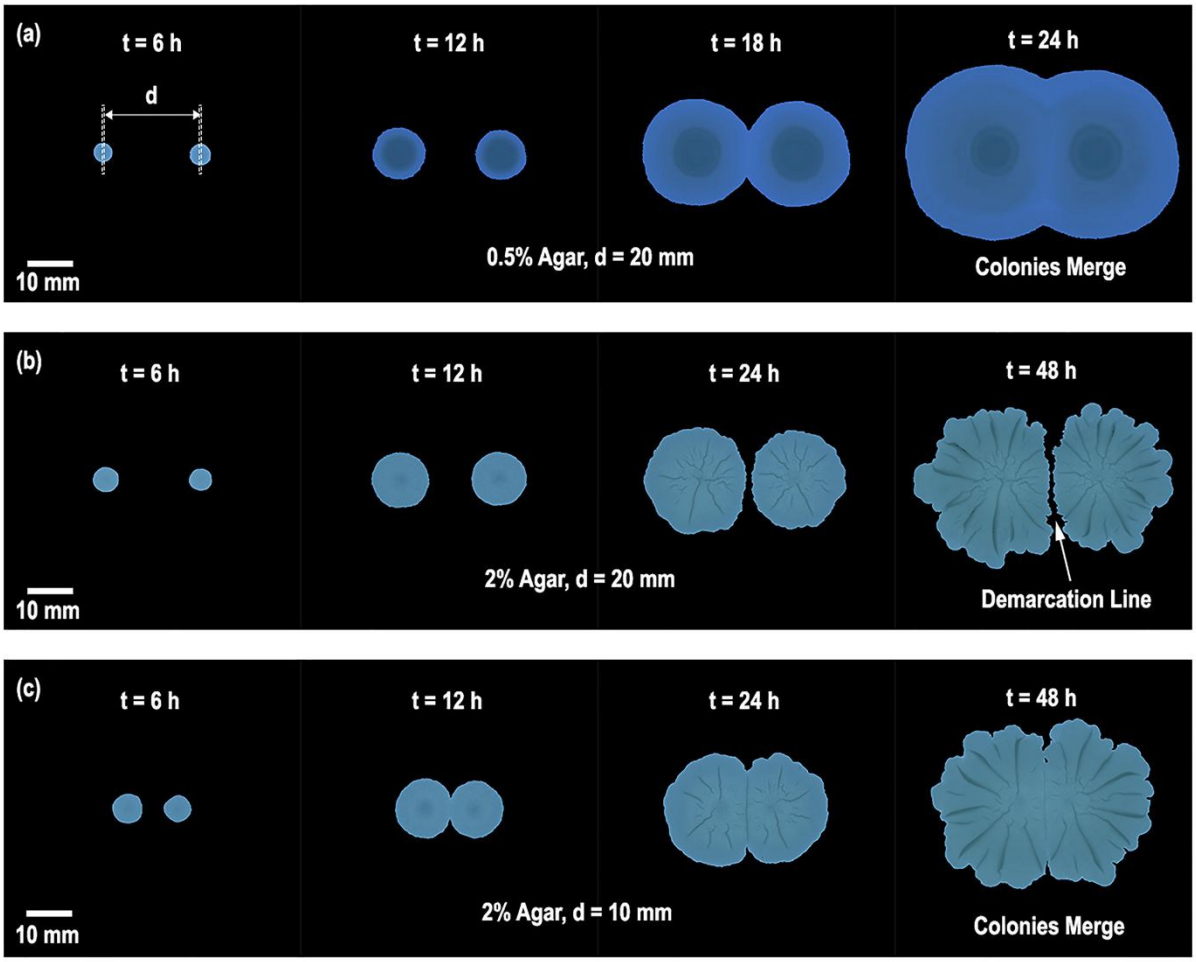

Fig. 1. Time lapse images of interacting *B. subtilis* colonies. **(a)** Colonies separated by 20 mm growing on 0.5% agar growth medium merge without forming a DL. **(b)** With the same initial separation, on 2% agar, the colonies are seen to form a distinct DL. **(c)** When the colonies are brought closer at d = 10 mm on 2% agar, no DL is observed.

View Article Online
DOI: 10.1039/C9SM00794F

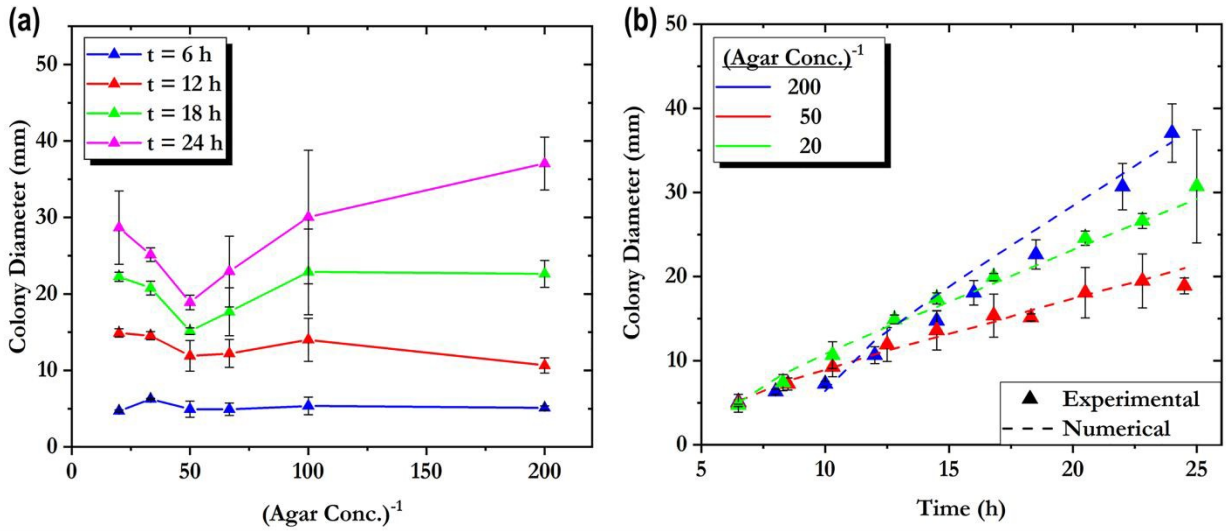

Fig. 2. Growth of single *B. subtilis* colony on agar-based growth medium. **(a)** Colony diameter is plotted against the reciprocal of the agar concentration at separate times. **(b)** Colony diameter is plotted against time for different agar concentrations. The dashed lines represent the numerical solution. In both figures, in the low agar regime (0.5% agar), the bacterial colonies grow much faster than at higher agar concentrations. The error bars indicated over the experimental data refers to the standard deviation in the collected data.

View Article Online
DOI: 10.1039/C9SM00794F

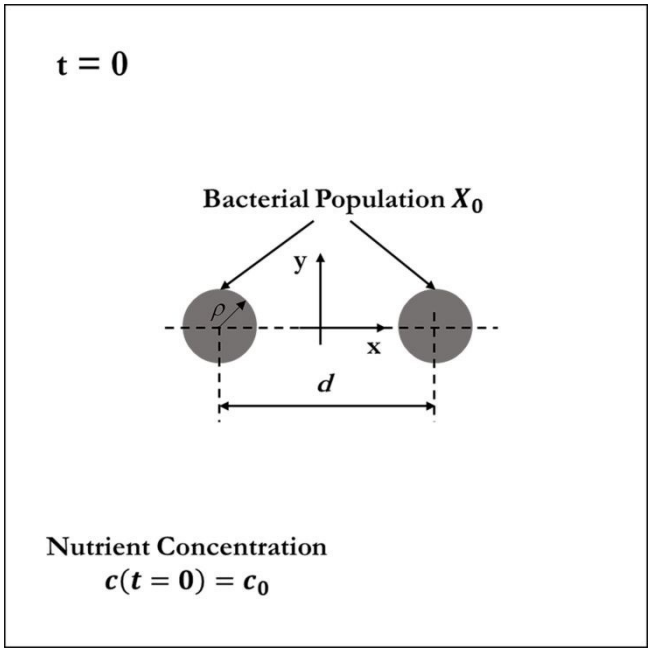

Fig. 3. Schematic showing the domain of numerical simulation at t = 0. The bacterial colonies are inoculated in the form of sessile drops of radius ρ (in grey) with initial bacterial population X_0. The initial nutrient concentration c_0 in the growth medium (in white) is uniformly distributed. The separation between the inoculated colonies is *d*.

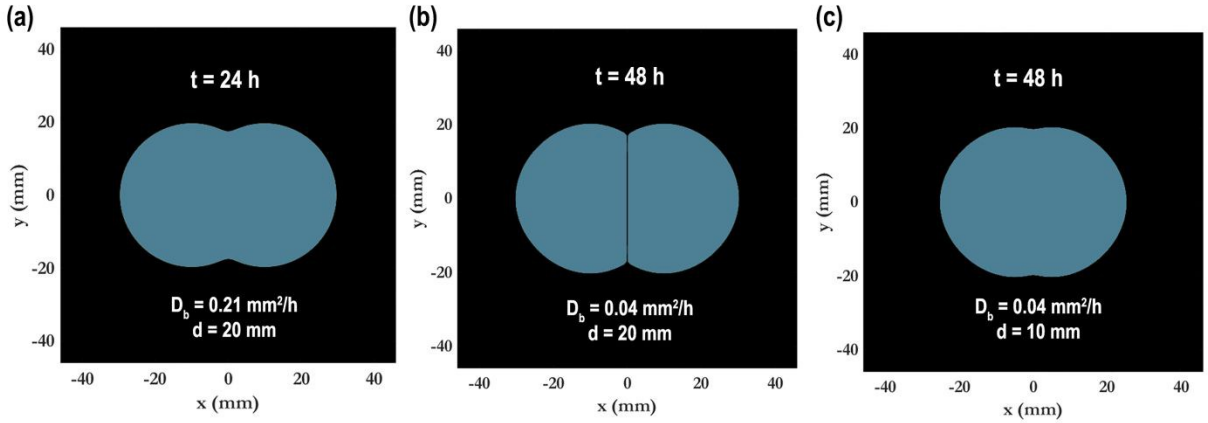

Fig. 4. Numerical simulation of *B. subtilis* colonies. **(a)** No DL is formed when the diffusion coefficient is large. Here $D_b = 0.21\ \text{mm}^2/\text{h}$ and initial separation $d = 20$ mm. **(b)** DL forms when the diffusion coefficient is reduced to $0.04\ \text{mm}^2/\text{h}$ while holding *d* constant. **(c)** If, however, *d* is lowered to 10 mm without changing the diffusion coefficient, merging occurs.

View Article Online
DOI: 10.1039/C9SM00794F

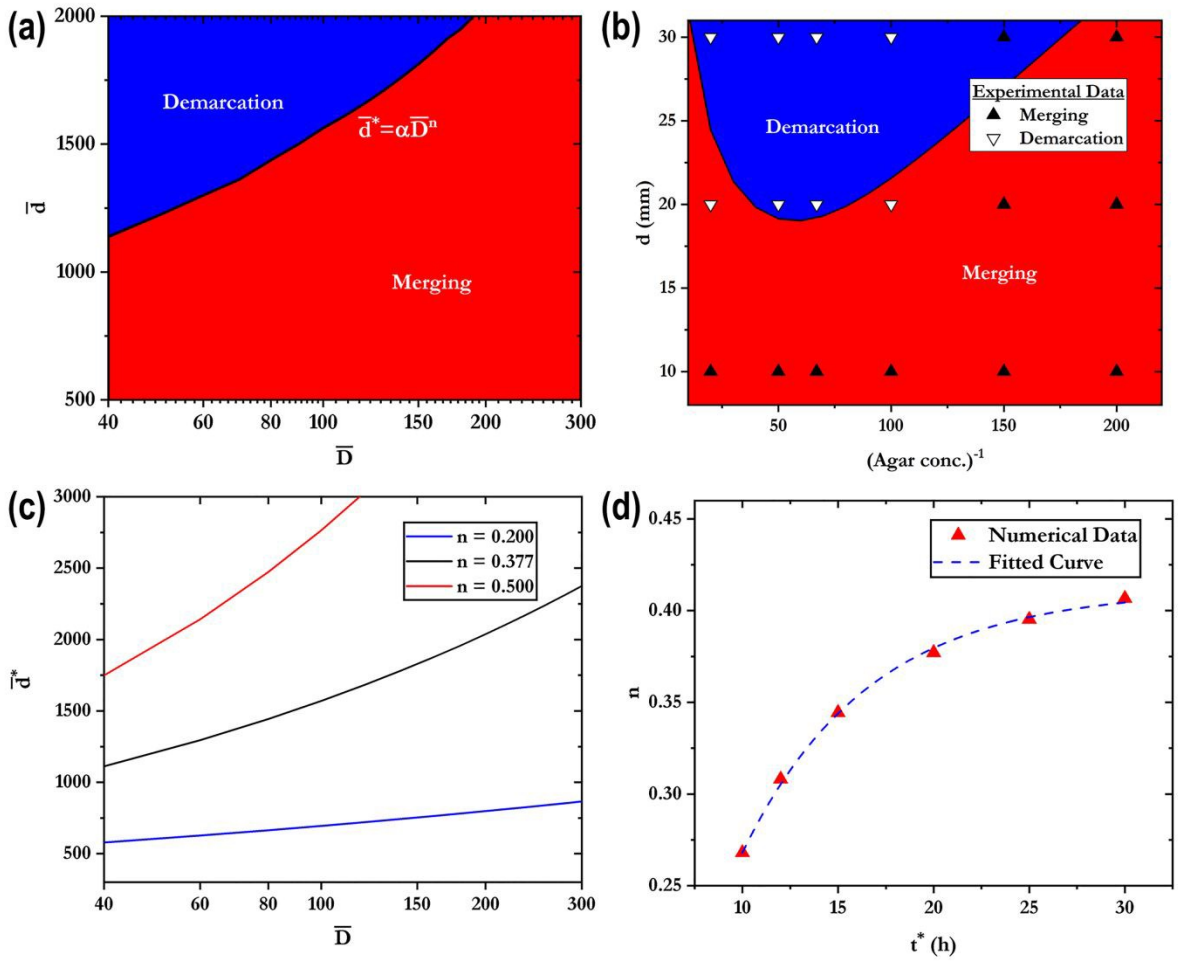

Fig. 5. Phase plots for DL formation in *B. subtilis* colonies. **(a)** Phase plot showing DL formation in a dimensionless variable space. **(b)** Corresponding dimensional phase plot for estimated parameters $g_0 = 4$/h and $D_c = 0.001$ mm^2/h. The dimensional numerical phase diagram is superposed with the experimental phase diagram. **(c)** Effect of the empirical index n on the critical dimensionless separation $\bar{d}^*$. $n = 0.377$ represents the numerical estimate. On the dimensionless phase diagram, for higher n, colonies merge, whereas for lower values, the interaction is DL dominated. **(d)** Influence of the reference time t^* on the empirical index n. The numerical data is fitted with an exponential function.

View Article Online
DOI: 10.1039/C9SM00794F

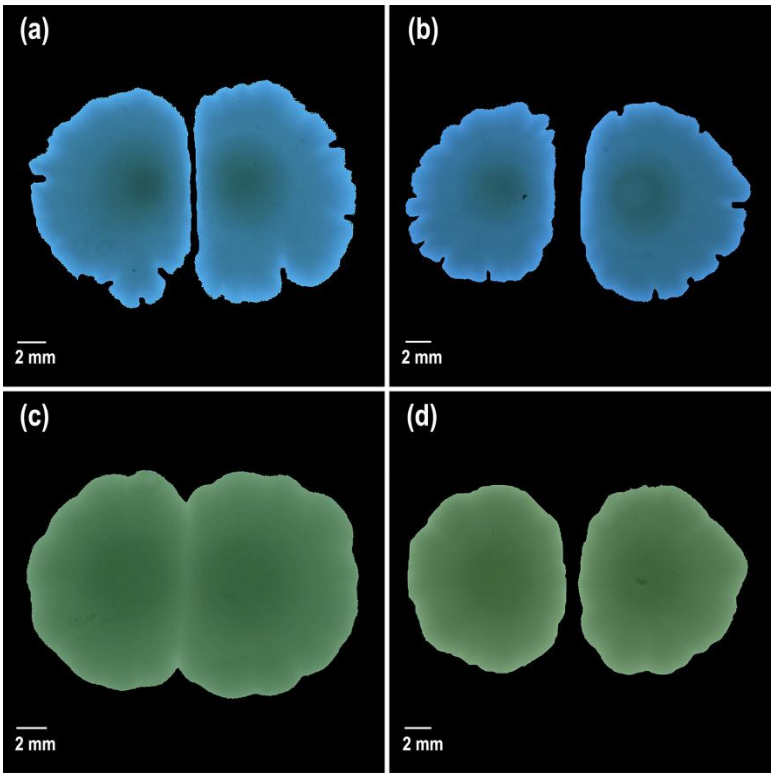

Fig. 6. Interaction patterns in *Escherichia coli* (**a** and **b**) and *Pseudomonas fluorescens* (**c** and **d**) on 1.5% and 0.5% agar media respectively. **(a)** In *E. coli* a DL forms when $d =$ 5 mm. **(b)** An DL also forms when $d =$ 10 mm. But in this case the gap between the interacting colony fronts is significant. **(c)** Merging occurs in *P. fluorescens* when the $d =$ 5 mm. **(d)** DL forms when $d =$ 10 mm. All images are taken 7 days post inoculation.

View Article Online
DOI: 10.1039/C9SM00794F

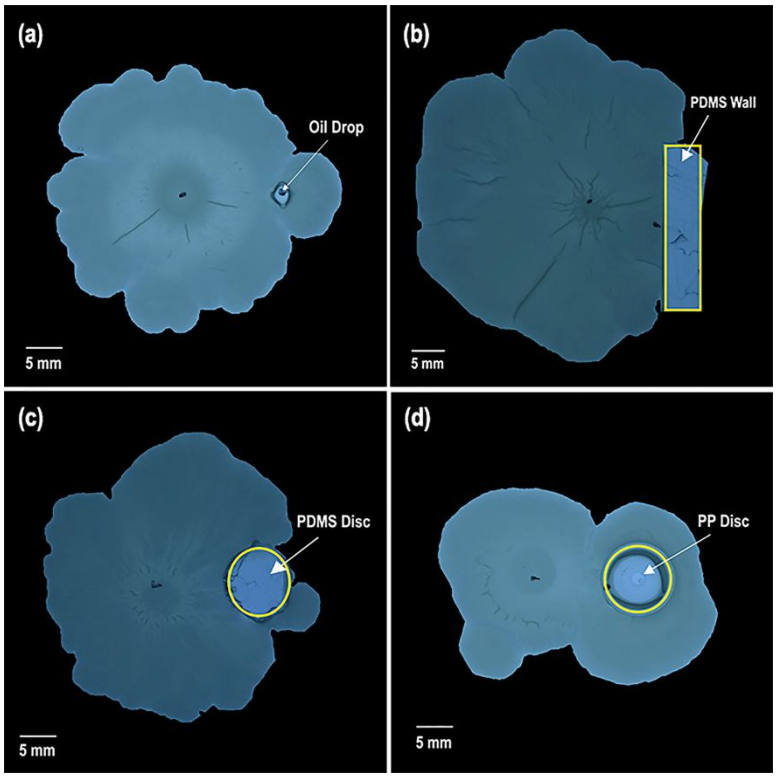

Fig. 7. Interaction of *B. subtilis* colonies with liquid and solid substrates produces no DL under similar conditions. **(a)** Colony interacting with sessile castor oil droplet. The colony grows around the oil droplet without any DL formation. Image corresponds to 78 hours post inoculation. **(b)** Approaching sibling colony front is simulated with a solid PDMS wall. The colony grows till the edge of the solid wall but do not form any DL near the flat solid surface of the wall. Image was taken 48 hours after inoculation. **(c)** A PDMS disc is used as a simulacrum for a sibling colony. In this case also, the colony does not form a DL but grows around the solid disc. Image was taken 48 hours after inoculation. **(d)** Like the PDMS disc, the colony reaches and grows around a PP disc. Image was taken 28 hours after inoculation. All four experiments were performed on 1.5% agar media.

View Article Online
DOI: 10.1039/C9SM00794F

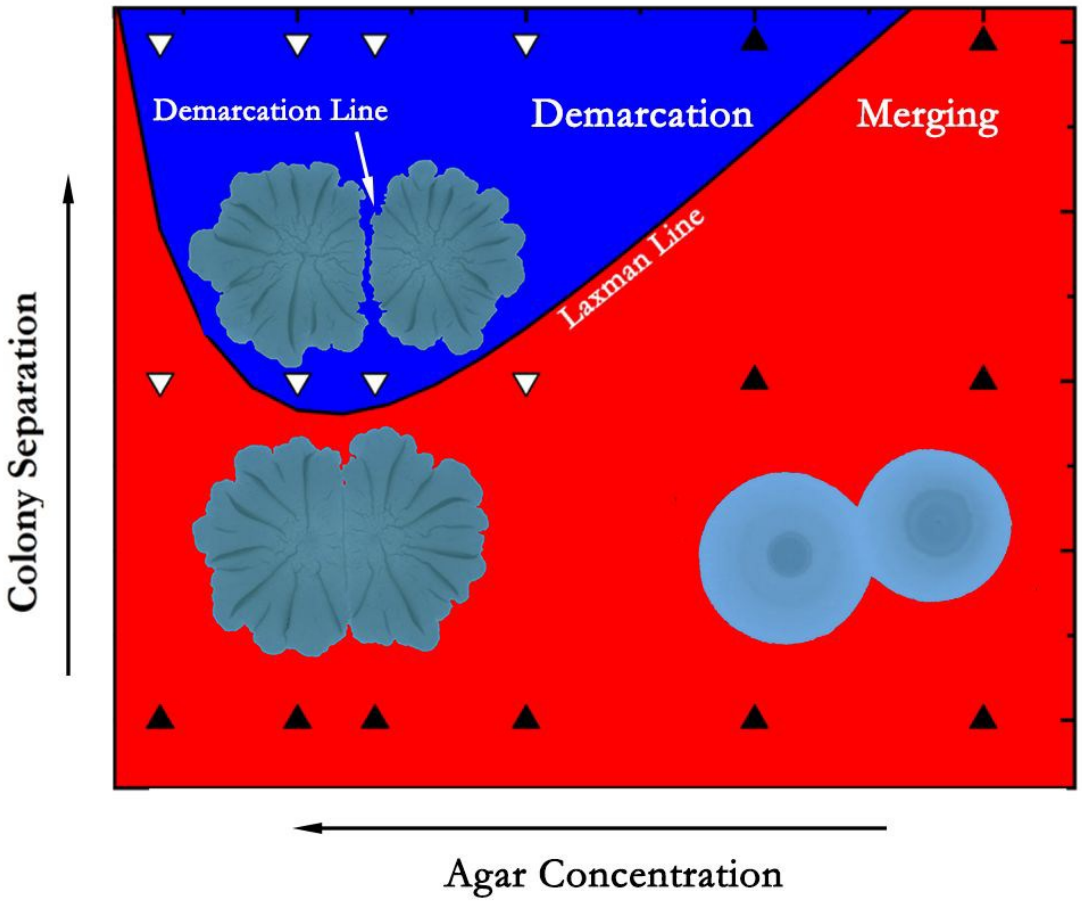

Sibling *Bacillus subtilis* colonies interact by demarcation (enemy) or merging (family), the regimes being separated by the Laxman line.